

# Direct demonstration of the two-phonon structure of the $J^\pi = 1_{4742\text{ keV}}^-$ state of $^{88}\text{Sr}$

J. Isaak,<sup>1,\*</sup> D. Savran,<sup>2</sup> N. Pietralla,<sup>1</sup> N. Tsoneva,<sup>3,4,†</sup> A. Zilges,<sup>5</sup>  
K. Eberhardt,<sup>6</sup> C. Geppert,<sup>6</sup> C. Gorges,<sup>6</sup> H. Lenske,<sup>4</sup> and D. Renisch<sup>7,8</sup>

<sup>1</sup>*Technische Universität Darmstadt, Department of Physics,  
Institute for Nuclear Physics, 64289 Darmstadt, Germany*

<sup>2</sup>*GSI Helmholtzzentrum für Schwerionenforschung GmbH, 64291 Darmstadt, Germany*

<sup>3</sup>*Extreme Light Infrastructure (ELI-NP), Horia Hulubei National Institute for R & D  
in Physics and Nuclear Engineering (IFIN-HH), 077125 Bucharest-Magurele, Romania*

<sup>4</sup>*Institut für Theoretische Physik, Universität Gießen,  
Heinrich-Buff-Ring 16, D-35392 Gießen, Germany*

<sup>5</sup>*Institut für Kernphysik, Universität zu Köln, 50937 Köln, Germany*

<sup>6</sup>*Forschungsreaktor TRIGA Mainz, Johannes Gutenberg-Universität Mainz, 55128 Mainz, Germany*

<sup>7</sup>*Department Chemie - Standort TRIGA, Johannes Gutenberg-Universität Mainz, 55128 Mainz, Germany*

<sup>8</sup>*Helmholtz Institut Mainz, 55128 Mainz, Germany*

(Dated: November 3, 2023)

We have studied the decay pattern of the  $J^\pi = 1_{4742\text{ keV}}^-$  state of  $^{88}\text{Sr}$  to probe its quadrupole-octupole coupled two-phonon structure. In particular, a unique fingerprint to prove the two-phonon nature is the  $E2$  decay strength of the  $1_{4742\text{ keV}}^- \rightarrow 3_1^-$  transition into the one-octupole-phonon state.  $\gamma$ -ray spectroscopy was performed after the  $\beta$ -decay of  $^{88}\text{Rb}$  to obtain the necessary sensitivity for this weak-intensity decay branch. Sufficient amounts of  $^{88}\text{Rb}$  ( $T_{1/2} = 17.8$  min) were produced by neutron activation of natural Rb in the TRIGA Mark II reactor. The results show that the  $B(E2)$  value of the  $1_{4742\text{ keV}}^- \rightarrow 3_1^-$  transition is equal to the  $B(E2)$  of the  $2_1^+ \rightarrow 0_1^+$  transition, directly demonstrating the quadrupole-octupole coupled two-phonon nature of the  $1^-$  state. A comparison of the results with energy-density functional plus quasiparticle-phonon model calculations shows remarkable agreement, corroborating this assignment.

## I. INTRODUCTION

Low-lying collective excitations of vibrational nuclei near shell closures are of particular interest for nuclear physics because atomic nuclei represent prime examples of strongly-coupled mesoscopic many-body quantum systems where collective vibrational excitations [1], frequently addressed as *phonons*, compete with single-particle excitations at low energy. Since the 1950s, there has been an intriguing question of how phonon excitations can couple to multi-phonon structures and thereby serve as building blocks for nuclear structure (see, e.g., [2] and references therein). Prime examples in even-even nuclei are the low-lying  $2^+$  and  $3^-$  states that are described by quadrupole and octupole phonon oscillations of the nuclear surface, respectively. The nature of a one-phonon state is described by the coherent superposition of particle-hole (p-h) excitations built on the ground state, while two-phonon states are composed of 2p-2h excitations built on the ground state with a similar generalization for multi-phonon states. In a simple phonon-coupling picture, phonons can couple to multi-phonon quantum states forming multiplets with the same structure and correlated decay properties. In a purely harmonic oscillator, two phonon states occur at an excitation energy corresponding to the sum energy of the constituent phonons. Deviations from that energy es-

imate are addressed as anharmonicities. Coupling of identical phonons based on the same single-particle excitations, e. g.  $(2^+ \otimes 2^+)$  [3–5] or  $(3^- \otimes 3^-)$  [6, 7], may lead to strong anharmonicities due to Pauli blocking effects. In contrast, Pauli blocking can be partly avoided by coupling different phonons, i. e., inhomogeneous phonon coupling [8] when the constituent phonons exhibit different single-particle structures. In leading order, the distortions are expected to be small in such inhomogeneous multi-phonon states and, thus, allow for a stringent test of the simple multi-phonon picture of collective low-lying excitations, both, in terms of anharmonicities and of purity of the multi-phonon wave functions. One prominent example of such an inhomogeneous phonon coupling is the quadrupole-octupole two-phonons excitations  $(2^+ \otimes 3^-)$  forming a quintuplet of nuclear levels with spin-parity quantum numbers  $J^\pi = 1^-, 2^-, 3^-, 4^-,$  and  $5^-$  [9–11].

The criteria for the solid experimental identification of vibrational multi-phonon states are currently still under debate [5, 12]. Lacking other experimental information, the excitation energy of the multi-phonon candidate states has often been considered for a multi-phonon criterion because it is expected to be close to the sum energy of the constituent phonons when assuming their harmonic coupling. This criterion is, however, weak because anharmonicities lead to deviations from this expectation and nuclear levels with different structure that, for any reason, may coincide with the sum energy, can erroneously be misinterpreted as multi-phonon states although they are not. Instead, the decisive signatures

\* jisaak@ikp.tu-darmstadt.de

† nadia.tsoneva@eli-np.ro

for multi-phonon structures are the collective strengths of the corresponding phonon-annihilating decay transitions that should correlate to the strengths of the ground-state decays of the corresponding one-phonon states. Anharmonicities observed for multi-phonon states may be caused by the influence of the underlying single-particle degree of freedom. Hence, the clear establishment of multi-phonon states and the thorough study of their properties provide information on the interplay of the collective and single-particle degrees of freedom in atomic nuclei.

The scope of the present work is focused on the investigation of the structure of the candidate for the quadrupole-octupole coupled  $J^\pi = 1_{2ph}^-$  state of  $^{88}\text{Sr}$ . Following the above mentioned signatures of a two-phonon state, the excitation energy is expected at  $E(1_{2ph}^-) \approx E(2_1^+) + E(3_1^-) = 1836 \text{ keV} + 2734 \text{ keV} = 4570 \text{ keV}$ . The method of Nuclear Resonance Fluorescence (NRF) has proven a powerful tool for searching for  $1_{2ph}^-$  states of vibrational nuclei [8, 13–20]. Previous NRF studies have identified the  $1^-$  state at 4742 keV to be the best candidate for the  $1_{2ph}^-$  state of this nucleus [21–23]. However, for a decisive identification, the reduced decay strengths of a harmonically coupled two-phonon  $1_{2ph}^-$  state have to fulfill the following relations:

$$B(E3, 1_{2ph}^- \rightarrow 2_1^+) = B(E3, 3_1^- \rightarrow 0_1^+) \quad (1)$$

$$B(E2, 1_{2ph}^- \rightarrow 3_1^-) = B(E2, 2_1^+ \rightarrow 0_1^+) \quad (2)$$

It is experimentally challenging to determine the  $E3$  contribution in the  $1_{2ph}^- \rightarrow 2_1^+$  decay, due to the dominant competition by  $E1$  multipolarity. The situation is different for the  $1_{2ph}^- \rightarrow 3_1^-$  transition, since the  $E2$  decay associated with the corresponding annihilation of the constituent quadrupole phonon is the leading multipolarity and a potential  $M3$  multipole admixture is subdominant. Using the value for  $B(E2, 2_1^+ \rightarrow 0_1^+) = 176(9) \text{ e}^2 \text{ fm}^4$  (adopted from [24]) and the ground-state transition strength of the  $1_{2ph}^-$  state (adopted from [23]), one expects a branching ratio of  $\Gamma(1_{2ph}^- \rightarrow 3_1^-) / \Gamma(1_{2ph}^- \rightarrow 0_1^+) = 0.034(5)$ . The measurement of branching ratios in the regime of a few percent is challenging in NRF experiments due to the rapidly increasing low-energy background originating from nonresonant photon scattering off the target. Some of us performed NRF experiments on  $^{88}\text{Sr}$  with quasi-monochromatic photon beams, but were unable to observe the 2008-keV  $\gamma$ -ray transition from the  $1_{2ph}^-$  state to the  $3_1^-$  state above background [21, 22].

An alternative approach to photon scattering experiments for the study of decay properties of excited states is off-beam  $\gamma$ -ray spectroscopy following  $\beta$ -decay after neutron activation. In contrast to in-beam experiments, activity measurements have the advantage of a significantly suppressed low-energy  $\gamma$ -ray background enabling the observation of weak transitions. Therefore, the neutron activation of  $^{87}\text{Rb}$  was exploited to populate excited states of  $^{88}\text{Sr}$  via  $\beta$  decay from  $^{88}\text{Rb}$ . The corresponding

$Q(\beta^-) = 5312 \text{ keV}$  is sufficiently high to allow the population of the candidate  $1_{2ph}^-$  two-phonon state at 4742 keV and study its decay behavior. Indeed the ground-state decay of the 4742 keV  $1_{2ph}^-$  state was observed in the  $\beta$ -decay of  $^{87}\text{Rb}$  in previous experiments [25, 26]. However, other decay channels were not observed due to the limited counting statistics of previous measurements. Therefore, we performed a new experiment with much higher sensitivity at the TRIGA Mark II reactor at Johannes Gutenberg-Universität Mainz.

This Letter is organized as follows. In the next section, the details on the neutron-activation measurement at TRIGA Mark II are given and the analysis of the activated  $^{87}\text{Rb}$  sample is presented. We then discuss the results for  $^{88}\text{Sr}$  in comparison to other nuclei before the Letter is concluded.

## II. EXPERIMENT & ANALYSIS

The neutron-activation experiment was conducted at the TRIGA Mark II research reactor at Johannes Gutenberg-Universität Mainz [27, 28]. The TRIGA Mainz is a light water cooled reactor using an alloy of uranium, zirconium, and hydrogen ( $U_{0.03}Zr_{0.97}H_1$ ) as fuel material. The uranium is enriched to below 20% in  $^{235}\text{U}$ . At the chosen irradiation position a neutron flux of about  $10^{12}$  neutrons per  $\text{cm}^2\text{s}$  is achieved at 100 kW reactor power.

Four samples with 500 ml of  $\text{RbNO}_3$  solution with a concentration of 100 mg/ml in natural Rb were irradiated for 30 min each, resulting in an activity of about 5.7 MBq of  $^{88}\text{Rb}$ , each. After a short waiting and transport time, the samples were placed in front of a high-purity germanium (HPGe) detector with a photo-peak efficiency at 1.33 MeV of 90% relative to an  $3'' \times 3''$  NaI detector. The detector is housed in a massive lead and copper shielding in order to reduce contributions of natural background. For the counting measurement, the samples were placed in an aluminum cylinder with a wall thickness of 9.13 mm in order to stop the electrons emitted in the beta decays. The setup allows to change the detector-to-sample distances in steps of 2 cm up to a maximum distance of 24 cm. The time for a single counting measurement was set to 5 min. Due to the short half-life of  $^{88}\text{Rb}$  of about 17.8 min, the overall count rate in the HPGe detector drops rapidly within a few minutes. In order to compensate for the reduced activity, the target was moved closer to the detector in steps of 2 cm when at the end of a counting measurement run the count rate dropped below 3 kcps (kilo counts per second). The closest detector-to-sample distance used was 6 cm to avoid considerable summing effects, which would become significant at even shorter distances. Summing effects are taken into account in the analysis using an iterative procedure with GEANT simulations, discussed in more detail below.

Figure 1 displays the summed  $\gamma$ -ray spectrum obtained

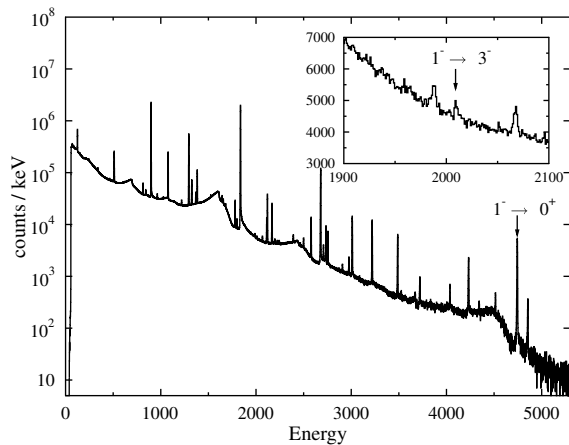


FIG. 1. Summed  $\gamma$ -ray spectrum of all four neutron-activation measurements taken with the HPGe detector. The ground-state decay of the candidate for the  $1_{2ph}^-$  state is marked with an arrow. The inset shows the region of interest for the  $1_{2ph}^- \rightarrow 3_1^-$  transition.

for all neutron-activation runs taken with the four samples. The dominant peaks belong to the beta decay of  $^{88}\text{Rb}$ , only small contributions of  $^{86}\text{Rb}$ ,  $^{24}\text{Na}$  and natural background are observed. The decay of the  $1^-$  state of interest at 4742.5 keV to the ground state is the dominant peak at higher energies. In total 29604(175) counts were collected in this transition, resulting in a statistical uncertainty of about 0.6%. The inset of Fig. 1 depicts the energy region of the expected  $1_{2ph}^- \rightarrow 3_1^-$  transition at 2008.3 keV, which is clearly visible above background with 2246(49) counts in total. Also the decay into the  $2_1^+$  and the  $2_2^+$  states is observed, which was known already from [23]. The branching ratio

$$b_f = \frac{A_{1^- \rightarrow f} / \epsilon(E_{1^-} - E_f)}{A_{1^- \rightarrow 0_1^+} / \epsilon(E_{1^-})} \quad (3)$$

represents the decay intensity from the  $1_{2ph}^-$  state to a state  $f$  at excitation energy  $E_f$  relative to its ground-state decay. The corresponding peak areas determined from the  $\gamma$ -ray spectrum given in Fig. 1 are  $A_{1^- \rightarrow f}$  and  $A_{1^- \rightarrow 0_1^+}$ , while the photo-peak detection efficiencies are denoted as  $\epsilon(E_{1^-} - E_f)$  and  $\epsilon(E_{1^-})$ , respectively. The efficiency ratio in Eq. (3) is obtained from a GEANT4 simulation [29–31] of an isotropically emitting  $\gamma$ -ray source placed in the experimental setup at detector-to-sample distances corresponding to the ones used in the actual measurements. In order to check the accuracy of the simulation, measurements with a  $^{56}\text{Co}$  source were conducted at 6 cm and 16 cm, respectively. The  $^{56}\text{Co}$  source was placed in the same aluminum cylinder as the Rb samples. The result of the simulation of the photo-peak efficiency for the two corresponding distances of 6 cm and 16 cm is shown in Fig. 2. The experimental data points extracted from the  $^{56}\text{Co}$  measurement are scaled to the simulation, because the activity of the source is not

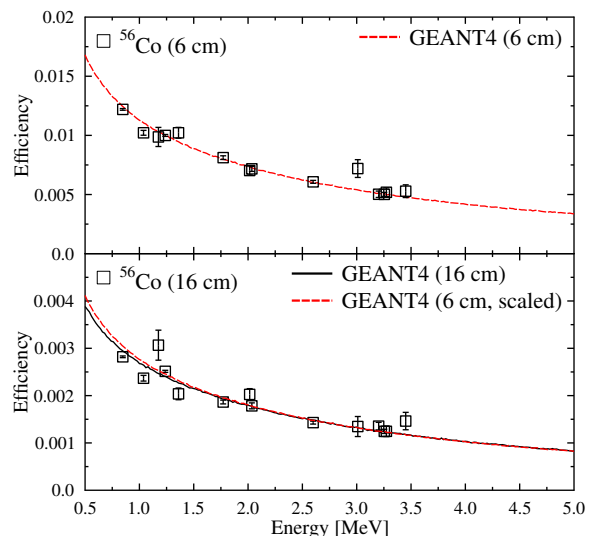


FIG. 2. Simulated photo-peak efficiencies for detector-to-sample distances of 6 cm (upper panel) and 16 cm (lower panel), respectively. The values measured with  $^{56}\text{Co}$  are scaled to the simulations. For comparison of the energy dependence at different distances the result of the simulation for 6 cm is scaled and plotted in the lower panel.

known with sufficient accuracy. Since the determination of the branching ratios  $b_f$  relies on the relative efficiencies only, it is sufficient to benchmark the energy dependence of the simulated photo-peak efficiency against the  $^{56}\text{Co}$  measurements. The comparison of the results shows that the variation of the energy dependence is weak for the two distances, especially for  $\gamma$ -ray energies above 1.5 MeV, which is the relevant energy region for the present analysis. To quantify the accuracy of the simulations with respect to the scaled  $^{56}\text{Co}$  data points, the weighted (external) uncertainty of the fit is calculated, which accounts for the spread of the data about the fit. For the two distances of 6 cm and 16 cm, relative weighted uncertainties of 0.75% and 1.37% are determined, respectively, which illustrates the good agreement of the simulated energy dependence of the photo-peak efficiency to the experimental values.

At the closest distance of 6 cm, the total detection probability, i.e. that any amount of energy is deposited in the detector, for a 2 MeV  $\gamma$ -ray is about 3.7%. Thus, summing effects of  $\gamma$ -rays within the cascades of the decay of the  $1_{2ph}^-$  state can play a role on that level. In order to account for this, the decay of the  $1_{2ph}^-$  state including the cascade transitions are simulated using the same GEANT4 simulation. The resulting intensities are compared to the experimental results in an iterative procedure: In the first step the branching ratios determined from experiment using Eq. (3) are used as input for the simulation of the cascades. The intensities obtained from this simulation are then compared to the experimental ones and a new set of branching ratios are determined to be used in the next iteration step. This procedure

TABLE I. Branching ratios  $b_f$  for the observed decay channels of the  $1_{2ph}^-$  state of  $^{88}\text{Sr}$  at 4742.4 keV to the  $2_1^+$ ,  $3_1^-$ , and  $2_2^+$  states extracted from the present data. The  $\gamma$ -ray transition energy, the excitation energy of the final state and its spin-parity quantum number are given by  $E_\gamma$ ,  $E_f$ , and  $J_f^\pi$ , respectively.

| $E_\gamma$ [keV] | $E_f$ [keV] | $J_f^\pi$ | $b_f$ [%] | $b_f^a$ [%] |
|------------------|-------------|-----------|-----------|-------------|
| 4742.4           | 0           | $0_1^+$   | 100.0(6)  | 100.0       |
| 2906.3           | 1836.1      | $2_1^+$   | 5.00(26)  | 4.4(19)     |
| 2008.3           | 2734.1      | $3_1^-$   | 3.72(29)  | -           |
| 1523.9           | 3218.5      | $2_2^+$   | 14.5(6)   | 22(9)       |

<sup>a</sup> computed from  $\Gamma_{1,2}/\Gamma$  values given in Table II of Ref. [23]

quickly converges to a final set of branching ratios for the different decay paths of the  $1_{2ph}^-$  state of interest.

Repeating this analysis using simulations at different distances results in slightly different final branching ratios, since the effect of summing depends on the total detection efficiency. Thus, the different results have been averaged weighted with the amount of data taken at the corresponding distance.

### III. RESULTS & DISCUSSION

The experimentally determined branching ratios  $b_f$  are summarized in Table I. With the present experiment, the uncertainties of the decay branching ratios to the  $2_{1,2}^+$  states and to the  $3_1^-$  state are improved by one order of magnitude enabling a determination of the ground-state branching ratio  $\Gamma_0/\Gamma = 0.811(5)$  of the  $1_{2ph}^-$  state at 4742.4 keV to a precision of 0.6%, which is one order of magnitude smaller compared to the precision of about 7% reported in Ref. [23]. Using this precisely determined value for  $\Gamma_0/\Gamma$  and the literature value for  $\Gamma_0^2/\Gamma = 107(14)$  meV from NRF experiments with bremsstrahlung [23], one obtains  $B(E1, 1_{2ph}^- \rightarrow 0_1^+) = 1.18(16) \times 10^{-3} \text{e}^2 \text{fm}^2$  for the reduced  $E1$  transition strength to the ground state. See Table II for a summary of the properties of the  $1_{2ph}^-$  state.

Moreover, the direct transition from the  $1_{2ph}^-$  two-phonon candidate state to the  $3_1^-$  one-octupole phonon state at 2734.1 keV was observed in the present experiment with a branching ratio of  $b_f = 3.72(29)\%$  for the first time. Its measurement provides now the possibility to determine the corresponding  $E2$  decay rate. The resulting reduced  $E2$  transition strength amounts to  $B(E2, 1_{2ph}^- \rightarrow 3_1^-) = 186(28) \text{e}^2 \text{fm}^4$ . As discussed above, a strong  $E2$  transition from the  $1_{2ph}^-$  state to the  $3_1^-$  is expected. In the two-phonon interpretation, the  $E2$  decay strength is supposed to be equal to the quadrupole-phonon annihilation depopulating the  $2_1^+$  state. A comparison to the adopted value for  $B(E2, 2_1^+ \rightarrow 0_1^+) =$

TABLE II. Properties of the  $1_{2ph}^-$  state at 4742.4 keV. The ground-state branching ratio  $\Gamma_0/\Gamma$ , ground-state transition width  $\Gamma_0$ , total width  $\Gamma$ , and the reduced ground-state transition strength  $B(E1, 1_{2ph}^- \rightarrow 0_1^+)$  are determined using the branching ratios given in Table I.

| $\Gamma_0^2/\Gamma^a$<br>[meV] | $\Gamma_0/\Gamma$ | $\Gamma_0$<br>[meV] | $\Gamma$<br>[meV] | $B(E1, 1^- \rightarrow 0_1^+)$<br>[ $10^{-3} \text{e}^2 \text{fm}^2$ ] |
|--------------------------------|-------------------|---------------------|-------------------|--|
| 107(14)                        | 0.811(5)          | 132(17)             | 163(21)           | 1.18(16)   |

<sup>a</sup> Value computed from  $g\Gamma_0^2/\Gamma = 322(42)$  meV given in Table I of Ref. [23] using  $g = 3$ .

$176(9) \text{e}^2 \text{fm}^4$  from Ref. [24] yields a ratio of:

$$\frac{B(E2, 1^- \rightarrow 3_1^-)}{B(E2, 2_1^+ \rightarrow 0_1^+)} = 1.06(17) \quad (4)$$

This result is in excellent agreement with the interpretation of the  $1_{2ph}^-$  state as a quadrupole-octupole coupled two-phonon state.

The experimental observations agree with predictions of the energy-density functional (EDF) and quasiparticle-phonon model (QPM) [32]. The building blocks of the QPM model basis are the quasiparticle-random-phase approximation (QRPA) phonons, which are superpositions of two-quasiparticle creation and annihilation operators [33]. The wave function of an excited QPM state is treated as a superposition of one-, two-, and three-phonon components, which in this case result from the coupling of  $J^\pi = 1^\pm - 7^\pm$  QRPA phonons and excitation energies up to the experimental endpoint excitation energy of the residual nucleus. For the dipole excitations, one-phonon states up to  $E_x = 25$  MeV are additionally considered, so that the pygmy dipole resonance (PDR) and the isovector giant dipole resonance (GDR) contribution to the  $E1$  transitions of the low-lying  $1^-$  states are explicitly taken into account avoiding the consideration of effective charges. Multi-phonon components in the wave function lead to violation of the Pauli principle. To account for it properly, we used the exact commutation relations between the phonon creation and annihilation operators.

QPM transition operators have harmonic and anharmonic parts and can therefore consider transitions beyond the quasi-boson approximation. Namely, the harmonic part gives the contribution arising from transitions between components in the wave function that differ by one phonon, and the anharmonic part couples components each with the same number of phonons or between those that differ by an even number of phonons [34]. In case of decay of the first  $1^-$  state to the ground state, the later one couples the two-phonon components of the first  $1^-$  state to the ground state and thus allows the description of this  $E1$  transition.

In the QPM calculations, two  $1^-$  states are obtained below 6 MeV. The wave function of the calculated  $1_1^-$  state contains about 90% of the  $(2_1^+ \otimes 3_1^-)$  component and 7% of the  $1_3^-$  QRPA state, which is an almost pure neutron QRPA state associated with the excitation of the

TABLE III. Comparison of experimental results to theoretical calculations within the QPM for  $^{88}\text{Sr}$ .

|  | Experiment | QPM  |
|--|------------|------|
| $E_x(1_1^-)$ [keV]                       | 4742       | 4603 |
| $E_x(2_1^+)$ [keV]                       | 1836       | 1830 |
| $E_x(3_1^-)$ [keV]                       | 2734       | 2760 |
| $B(E1, 1_1^- \rightarrow 0_1^+)$ [mW.u.] | 0.93(12)   | 0.96 |
| $B(E2, 1_1^- \rightarrow 3_1^-)$ [W.u.]  | 8.0(12)    | 8.1  |
| $B(E2, 2_1^+ \rightarrow 0_1^+)$ [W.u.]  | 7.6(4)     | 8.0  |

PDR mode in this nucleus [35, 36]. Furthermore, due to the one-phonon and two-phonon components in the structure of the  $1_1^-$  state, anharmonicity effects shift the excitation energy of the state to lower excitation energies with respect to the pure harmonic expectation energy resulting from the sum of the energies of the QRPA  $2_1^+$  and  $3_1^-$  states.

Thus, the theoretical results support the picture of a dominant contribution of quadrupole and octupole phonons in the wave function of the  $1_1^-$  state with equal  $B(E2)$  values in the  $1_1^- \rightarrow 3_1^-$  and  $2_1^+ \rightarrow 0_1^+$  transitions, interpreted by the annihilation of the same quadrupole phonon, represented here by the  $2_1^+$  state with an  $E2$  transition strength of about 8 W.u. to the ground state. The  $1_2^-$  is dominated to 98 % by the  $(2_2^+ \otimes 3_1^-)$  component. It can be ruled out as a potential representation of the experimentally observed  $1_{2ph}^-$  state due to its calculated  $B(E2, 1_2^- \rightarrow 3_1^-) = 0.03$  W.u. which exhibits a two orders of magnitude smaller  $E2$  transition strength.

Theoretically, we identify the  $1_1^-$  state in the QPM calculations as the quadrupole-octupole coupled two-phonon state of interest for comparison with the experimental data. The computed transition strengths for the  $1_1^-$  and  $2_1^+$  states are in remarkable agreement to the experimental values and are summarized in Tab. III. The decay strengths for both the  $1_1^- \rightarrow 0_1^+$  and the  $1_1^- \rightarrow 3_1^-$  transitions are in excellent agreement to the measured data.

Experimental information on the  $B(E2, 1_{2ph}^- \rightarrow 3_1^-)/B(E2, 2_1^+ \rightarrow 0_1^+)$  ratio is very scarce and has been observed only for a few nuclei so far, namely  $^{40}\text{Ca}$  [37],  $^{142}\text{Nd}$  [38, 39],  $^{144}\text{Nd}$  [40], and  $^{144}\text{Sm}$  [38]. The corresponding measured  $B(E2)$  ratios are displayed in Fig. 3 a). The dashed line indicates 1.0, which is the expected ratio in an unperturbed phonon-coupling picture. A very good agreement with the two-phonon interpretation of the lowest-lying  $1^-$  states is observed in most cases while the  $B(E2)$  value for  $^{144}\text{Nd}$  lies slightly below the theoretical prediction for a pure two-phonon state. Moreover, the excitation energies of all of these  $1^-$  states lie within less than 10 % of the sum energy of the constituent one-phonon states with the only exception of  $^{40}\text{Ca}$  where the  $1_{2ph}^-$  state exhibits a slightly larger negative anharmonicity of -22 %; compare with Fig. 3 b). This appreciable overall agreement of the excitation energies of the

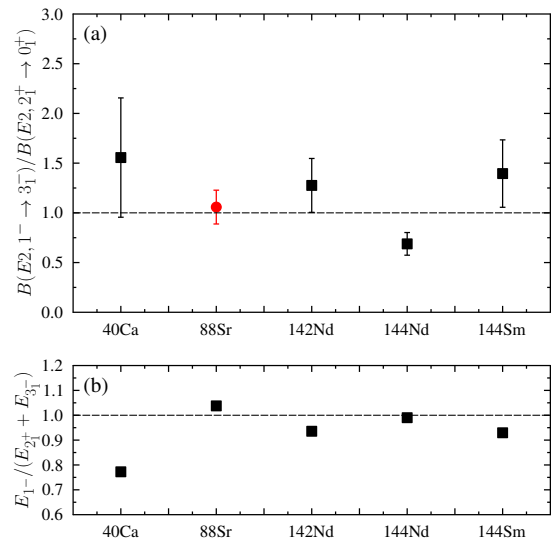


FIG. 3. Comparison of (a) the experimentally determined  $B(E2)$  value branching ratios for two-phonon  $1_{2ph}^-$  states in  $^{40}\text{Ca}$  [37],  $^{142}\text{Nd}$  [38, 39],  $^{144}\text{Nd}$  [40], and  $^{144}\text{Sm}$  [38] and (b) the corresponding excitation energies.

$1_{2ph}^-$  states, identified independently via their collective  $E2$  decay strengths of the quadrupole-phonon annihilating transitions as quite unperturbed two-phonon structures, with the sum energy of the one-phonon states underpins that their coupling seems to be fairly harmonic.

The fact, that the known lowest-lying  $1^-$  states of nuclei at and near shell closures in different mass regions ranging from  $A = 40$  to  $A = 88$  and  $A \approx 144$  show a similar behavior with respect to their decay properties, is clear evidence that two-phonon states are a general feature of atomic nuclei giving proof of the constituent quadrupole and octupole phonons as solid building blocks of multi-phonon nuclear structures.

#### IV. CONCLUSIONS

In summary, neutron-activation measurements were performed at the TRIGA Mark II reactor at Johannes Gutenberg-Universität Mainz to investigate the structure of the best candidate for the quadrupole-octupole coupled two-phonon  $1_{2ph}^-$  state at 4742 keV of  $^{88}\text{Sr}$ . The  $\gamma$ -decay branching ratios of the  $1_{2ph}^-$  state to the  $2_{1,2}^+$  and  $3_1^-$  states were measured with a precision of better than 8 % improving the existing literature values by about one order of magnitude. As a consequence, the  $\Gamma_0/\Gamma = 0.811(5)$  value of the dominant ground-state decay channel is determined to 0.6 % accuracy. The direct transition from the  $1_{2ph}^-$  to the  $3_1^-$  was observed for  $^{88}\text{Sr}$ . A comparison of the corresponding  $B(E2, 1_{2ph}^- \rightarrow 3_1^-)$  value to the ground-state decay strength of the  $2_1^+$  state,  $B(E2, 2_1^+ \rightarrow 0_1^+)$ , directly proves the  $1_{2ph}^-$  state as the

two-phonon member of the  $(2^+ \otimes 3^-)$  quintuplet. This assignment is in remarkable agreement with the predictions of the EDF+three-phonon QPM calculations.

While the  $E2$  decay strength to the  $3_1^-$  state is the decisive signature of a quadrupole-octupole coupled two-phonon state, additional criteria, apart from the excitation energy of the  $1_{2ph}^-$  state, were proposed for supporting such an identification [5]. For instance, transfer reactions were used to rule out two-phonon states, because they may be expected to possess small single- and two-nucleon transfer cross sections (see, e.g., Ref. [41]). Hence, high-resolution transfer-reaction experiments may help to shed more light on the microscopic structure of the  $1_{2ph}^-$  state at 4742 keV as a member of the quadrupole-octupole quintuplet of  $^{88}\text{Sr}$ .

Furthermore, extended systematic studies of the  $B(E2, 1^- \rightarrow 3_1^-)$  values of other  $1^-$  states in the 4 MeV to 6 MeV excitation-energy region of  $^{88}\text{Sr}$  can elucidate whether the excellent match with the  $B(E2, 2_1^+ \rightarrow 0_1^+)$  value is an exclusive property of the  $1_{2ph}^-$  state at 4742 keV or if other  $1^-$  states could exhibit similar, large decay strengths. An experimental program on the  $E2$  strength distribution of  $1^- \rightarrow 3^-$   $\gamma$ -ray transitions in vibrational nuclei is needed to clarify that question. Quasi-monochromatic beams of photons may be utilized for this task. They can provide a selective probe for the study of

dipole-excited states. Photonuclear reactions with quasi-monochromatic photon beams combined with a high-efficiency  $\gamma$ -ray coincidence setup have proven lately to be very well suited for systematic investigations of decay branchings of dipole-excited states in the order of a few percent [20, 37, 42–45] and systematic measurements of the distribution of  $B(E2; 1^- \rightarrow 3^-)$  values in selected vibrational key nuclei would be highly desirable.

## ACKNOWLEDGMENTS

The authors thank the entire staff of the TRIGA reactor in Mainz for the excellent experimental conditions and support during the project. Parts of the work were supported by the Deutsche Forschungsgemeinschaft (DFG, German Research Foundation) - Project-ID 499256822 - GRK 2891. J. I. and N. P. acknowledge support by the grant "Nuclear Photonics" within the LOEWE program of the State of Hesse and within the Research Cluster ELEMENTS (Project ID 500/10.006). N. T. acknowledges support by the contract PN 23.21.01.06 sponsored by the Romanian Ministry of Research, Innovation and Digitalization. A. Z. acknowledges support by the DFG (Contract No. ZI 510/10-1). H. L. is supported by DFG grant Le439/16. N. T. is grateful for the kind hospitality of the University of Giessen.

- 
- [1] A. Bohr, *Mat. Fys. Medd. Dan. Vid. Selsk.* **26** (1952).  
 [2] R. F. Casten, *Nuclear Structure from a Simple Perspective; 2st ed.* (Oxford Univ. Press, New York, NY, 1990).  
 [3] G. Scharff-Goldhaber and J. Weneser, *Phys. Rev.* **98**, 212 (1955).  
 [4] J. Kern, P. Garrett, J. Jolie, and H. Lehmann, *Nucl. Phys. A* **593**, 21 (1995).  
 [5] P. E. Garrett, J. L. Wood, and S. W. Yates, *Phys. Scr.* **93**, 34 (2018).  
 [6] M. Yeh, P. E. Garrett, C. A. McGrath, S. W. Yates, and T. Belgia, *Phys. Rev. Lett.* **76**, 1208 (1996).  
 [7] P. Kleinheinz, J. Styczen, M. Piiparinen, J. Blomqvist, and M. Kortelahti, *Phys. Rev. Lett.* **48**, 1457 (1982).  
 [8] N. Pietralla, *Phys. Rev. C* **59**, 2941 (1999).  
 [9] P. O. Lipas, *Nucl. Phys.* **82**, 91 (1966).  
 [10] P. Vogel and L. Kocbach, *Nucl. Phys. A* **176**, 33 (1971).  
 [11] N. A. Smirnova, N. Pietralla, T. Mizusaki, and P. Van Isacker, *Nuclear Physics A* **678**, 235 (2000).  
 [12] P. E. Garrett, T. R. Rodríguez, A. Diaz Varela, K. L. Green, J. Bangay, A. Finlay, R. A. E. Austin, G. C. Ball, D. S. Bandyopadhyay, V. Bildstein, S. Colosimo, D. S. Cross, G. A. Demand, P. Finlay, A. B. Garnsworthy, G. F. Grinyer, G. Hackman, B. Jigmeddorj, J. Jolie, W. D. Kulp, K. G. Leach, A. C. Morton, J. N. Orce, C. J. Pearson, A. A. Phillips, A. J. Radich, E. T. Rand, M. A. Schumaker, C. E. Svensson, C. Sumithrarachchi, S. Triambak, N. Warr, J. Wong, J. L. Wood, and S. W. Yates, *Phys. Rev. C* **101**, 044302 (2020).  
 [13] F. R. Metzger, *Phys. Rev. C* **14**, 543 (1976).  
 [14] F. R. Metzger, *Phys. Rev. C* **18**, 2138 (1978).  
 [15] F. R. Metzger, *Phys. Rev. C* **18**, 1603 (1978).  
 [16] R.-D. Herzberg, I. Bauske, P. von Brentano, T. Eckert, R. Fischer, W. Geiger, U. Kneissl, J. Margraf, H. Maser, N. Pietralla, H. Pitz, and A. Zilges, *Nucl. Phys.* **A592**, 211 (1995).  
 [17] U. Kneissl, H. H. Pitz, and A. Zilges, *Prog. Part. Nucl. Phys.* **37**, 349 (1996).  
 [18] W. Andrejtscheff, C. Kohstall, P. von Brentano, C. Fransen, U. Kneissl, N. Pietralla, and H. H. Pitz, *Phys. Lett. B* **506**, 239 (2001).  
 [19] C. Fransen, N. Pietralla, A. P. Tonchev, M. W. Ahmed, J. Chen, G. Feldman, U. Kneissl, J. Li, V. N. Litvinenko, B. Perdue, I. V. Pinayev, H. H. Pitz, R. Prior, K. Sabourov, M. Spraker, W. Tornow, H. R. Weller, V. Werner, Y. K. Wu, and S. W. Yates, *Phys. Rev. C* **70**, 044317 (2004).  
 [20] A. Zilges, D. Balabanski, J. Isaak, and N. Pietralla, *Progress in Particle and Nuclear Physics* **122**, 103903 (2022).  
 [21] N. Pietralla, V. N. Litvinenko, S. Hartman, F. F. Mikhailov, I. V. Pinayev, G. Swift, M. W. Ahmed, J. H. Kelley, S. O. Nelson, R. Prior, K. Sabourov, A. P. Tonchev, and H. R. Weller, *Phys. Rev. C* **65**, 047305 (2002).  
 [22] N. Pietralla, V. N. Litvinenko, S. Hartman, F. F. Mikhailov, I. V. Pinayev, G. Swift, M. W. Ahmed, J. H. Kelley, S. O. Nelson, R. Prior, K. Sabourov, A. P. Tonchev, and H. R. Weller, *Phys. Rev. C* **65**, 069901(E)

- (2002).
- [23] L. Käubler, H. Schnare, R. Schwengner, H. Prade, F. Döna, P. von Brentano, J. Eberth, J. Enders, A. Fitzler, C. Fransen, M. Grinberg, R.-D. Herzberg, H. Kaiser, P. von Neumann-Cosel, N. Pietralla, A. Richter, G. Rusev, C. Stoyanov, and I. Wiedenhöver, *Phys. Rev. C* **70**, 064307 (2004).
- [24] E. McCutchan and A. Sonzogni, *Nuclear Data Sheets* **115**, 135 (2014).
- [25] R. L. Bunting, W. L. Talbert, J. R. McConnell, and R. A. Meyer, *Phys. Rev. C* **13**, 1577 (1976).
- [26] H. Miyahara, A. Yoshida, G. Wurdiant, H. Nagata, and N. Marnada, *Applied Radiation and Isotopes* **56**, 163 (2002), proceedings of the Conference on Radionuclide Metrology and its Applications, ICRM'01.
- [27] K. Eberhardt and N. Trautmann, *IAEA Technical Reports Series* **455**, 537 (2007).
- [28] K. Eberhardt and C. Geppert, *Radiochimica Acta* **107**, 535 (2019).
- [29] S. Agostinelli, J. Allison, K. Amako, J. Apostolakis, H. Araujo, P. Arce, M. Asai, D. Axen, S. Banerjee, G. Barrand, F. Behner, L. Bellagamba, J. Boudreau, and *et al.*, *Nucl. Instr. Meth. Phys. Res. A* **506**, 250 (2003).
- [30] J. Allison, K. Amako, J. Apostolakis, H. Araujo, P. Arce Dubois, M. Asai, G. Barrand, R. Capra, S. Chauvie, R. Chytráček, G. A. P. Cirrone, G. Cooperman, G. Cosmo, G. Cuttone, G. G. Daquino, M. Donszelmann, M. Dressel, G. Folger, F. Foppiano, J. Generowicz, V. Grichine, S. Guatelli, P. Gumplinger, A. Heikkinen, I. Hrivnacova, A. Howard, S. Incerti, V. Ivanchenko, T. Johnson, F. Jones, T. Koi, R. Kokoulin, M. Kossov, H. Kurashige, V. Lara, S. Larsson, F. Lei, O. Link, F. Longo, M. Maire, A. Mantero, B. Mascialino, I. McLaren, P. Mendez Lorenzo, K. Minamimoto, K. Murakami, P. Nieminen, L. Pandola, S. Parlati, L. Peralta, J. Perl, A. Pfeiffer, M. G. Pia, A. Ribon, P. Rodrigues, G. Russo, S. Sadilov, G. Santin, T. Sasaki, D. Smith, N. Starkov, S. Tanaka, E. Tcherniaev, B. Tome, A. Trindade, P. Truscott, L. Urban, M. Verderi, A. Walkden, J. P. Wellisch, D. C. Williams, D. Wright, and H. Yoshida, *IEEE Transactions on Nuclear Science* **53**, 270 (2006).
- [31] J. Allison, K. Amako, J. Apostolakis, P. Arce, M. Asai, T. Aso, E. Bagli, A. Bagulya, S. Banerjee, G. Barrand, B. Beck, A. Bogdanov, D. Brandt, J. Brown, H. Burkhardt, P. Canal, D. Cano-Ott, S. Chauvie, K. Cho, G. Cirrone, G. Cooperman, M. Cortés-Giraldo, G. Cosmo, G. Cuttone, G. Depaola, L. Desorgher, X. Dong, A. Dotti, V. Elvira, G. Folger, Z. Francis, A. Galoyan, L. Garnier, M. Gayer, K. Genser, V. Grichine, S. Guatelli, P. Guèye, P. Gumplinger, A. Howard, I. Hrivnáčová, S. Hwang, S. Incerti, A. Ivanchenko, V. Ivanchenko, F. Jones, S. Jun, P. Kaitaniemi, N. Karakatsanis, M. Karamitros, M. Kelsey, A. Kimura, T. Koi, H. Kurashige, A. Lechner, S. Lee, F. Longo, M. Maire, D. Mancusi, A. Mantero, E. Mendoza, B. Morgan, K. Murakami, T. Nikitina, L. Pandola, P. Paprocki, J. Perl, I. Petrović, M. Pia, W. Pokorski, J. Quesada, M. Raine, M. Reis, A. Ribon, A. Ristić Fira, F. Romano, G. Russo, G. Santin, T. Sasaki, D. Sawkey, J. Shin, I. Strakovsky, A. Taborda, S. Tanaka, B. Tomé, T. Toshito, H. Tran, P. Truscott, L. Urban, V. Uzhinsky, J. Verbeke, M. Verderi, B. Wendt, H. Wenzel, D. Wright, D. Wright, T. Yamashita, J. Yarba, and H. Yoshida, *Nuclear Instruments and Methods in Physics Research Section A: Accelerators, Spectrometers, Detectors and Associated Equipment* **835**, 186 (2016).
- [32] N. Tsoneva and H. Lenske, *Physics of Atomic Nuclei* **79**, 885 (2016).
- [33] V. G. Soloviev, *Theory of Atomic Nuclei: Quasiparticles and Phonons* (Institute of Physics, Bristol, 1992).
- [34] V. Ponomarev, C. Stoyanov, N. Tsoneva, and M. Grinberg, *Nucl. Phys.* **635**, 470 (1998).
- [35] R. Schwengner, G. Rusev, N. Tsoneva, N. Benouaret, R. Beyer, M. Erhard, E. Grosse, A. R. Junghans, J. Klug, K. Kosev, H. Lenske, C. Nair, K. D. Schilling, and A. Wagner, *Phys. Rev. C* **78**, 064314 (2008).
- [36] R. Schwengner, R. Massarczyk, G. Rusev, N. Tsoneva, D. Bemmerer, R. Beyer, R. Hannaske, A. R. Junghans, J. H. Kelley, E. Kwan, H. Lenske, M. Marta, R. Raut, K. D. Schilling, A. Tonchev, W. Tornow, and A. Wagner, *Phys. Rev. C* **87**, 024306 (2013).
- [37] V. Derya, N. Tsoneva, T. Aumann, M. Bhihe, J. Endres, M. Gooden, A. Hennig, J. Isaak, H. Lenske, B. Löher, N. Pietralla, D. Savran, W. Tornow, V. Werner, and A. Zilges, *Phys. Rev. C* **93**, 034311 (2016).
- [38] M. Wilhelm, E. Radermacher, A. Zilges, and P. v. Brentano, *Phys. Rev. C* **54**, R449 (1996).
- [39] M. Wilhelm, S. Kasemann, G. Pascovici, E. Radermacher, P. von Brentano, and A. Zilges, *Phys. Rev. C* **57**, 577 (1998).
- [40] A. Sonzogni, *Nuclear Data Sheets* **93**, 599 (2001).
- [41] D. S. Jamieson, P. E. Garrett, V. Bildstein, G. A. Demand, P. Finlay, K. L. Green, K. G. Leach, A. A. Phillips, C. S. Sumithrarachchi, C. E. Svensson, S. Triambak, G. C. Ball, T. Faestermann, R. Hertenberger, and H.-F. Wirth, *Phys. Rev. C* **90**, 054312 (2014).
- [42] B. Löher, V. Derya, T. Aumann, J. Beller, N. Cooper, M. Duchene, J. Endres, E. Fiori, J. Isaak, J. Kelley, M. Knörzer, N. Pietralla, C. Romig, D. Savran, M. Scheck, H. Scheit, J. Silva, A. P. Tonchev, W. Tornow, H. Weller, V. Werner, and A. Zilges, *Nucl. Instr. Meth. Phys. Res. A* **723**, 136 (2013).
- [43] B. Löher, D. Savran, T. Aumann, J. Beller, M. Bhihe, N. Cooper, V. Derya, M. Duchene, J. Endres, A. Hennig, P. Humby, J. Isaak, J. Kelley, M. Knörzer, N. Pietralla, V. Ponomarev, C. Romig, M. Scheck, H. Scheit, J. Silva, A. Tonchev, W. Tornow, F. Wamers, H. Weller, V. Werner, and A. Zilges, *Phys. Lett. B* **756**, 72 (2016).
- [44] J. Isaak, D. Savran, B. Löher, T. Beck, M. Bhihe, U. Gayer, Krishichayan, N. Pietralla, M. Scheck, W. Tornow, V. Werner, A. Zilges, and M. Zweidinger, *Phys. Lett. B* **788**, 225 (2019).
- [45] J. Isaak, D. Savran, B. Löher, T. Beck, U. Friman-Gayer, Krishichayan, N. Pietralla, V. Y. Ponomarev, M. Scheck, W. Tornow, V. Werner, A. Zilges, and M. Zweidinger, *Phys. Rev. C* **103**, 044317 (2021).